The Effect of Heating-Cooling Process on Mode I Fracture Toughness of Rocks

Ahmad Jabari, Mehdi Hosseini*
Department of Mining Engineering, Imam Khomeini International University, Ghazvin

Received: October 2018 Revised: February 2019

Abstract

In cases such as explosion, fire, deep drilling and geothermal energy extraction, rocks are exposed to high temperatures influencing the rock toughness. Thus, the aim of this study is to investigate the effect of temperature on the fracture toughness of the rocks. In this study, the effect of temperature on the mode I fracture toughness is investigated. To this end, three-point bending tests were performed on semicircular specimens of four types of natural rocks including sandstone, limestone, tuff, andesite, and a series of concrete specimens to determine the fracture toughness. The specimens were first heated to 100, 200, 300, 500 and 700 °C. After reaching the desired temperatures, the specimens were cooled. A series of tests was performed on the specimens at ambient temperature (25 °C). The heating rate in the electric furnace was 15 °C/min in accordance with the temperature rise in fires. Petrographic studies and X-ray diffraction analysis (XRD) were performed to identify the composition of the rocks. Furthermore, the effective porosity and the weight loss of heated specimens were determined to

*Corresponding author mahdi_hosseini@ikiu.ac.ir

[DOR: 20.1001.1.22286837.1398.13.5.6.5]

study the behavior of rocks. Comparison of the test results indicated the higher impact of temperature on the fracture toughness of fine-grained rocks. In addition, the fracture toughness decreased by increasing the effective porosity and decreasing the weight loss. According to the results, the mode I fracture toughness of sandstone, tuff, limestone, andesite and concrete specimens underwent a heating-cooling cycle up to 700 $^{\circ}$C respectively decreased 45, 17, 44 and 9.5 and 37 percent compared with that of unheated specimens.

Keywords: Fracture toughness, mode I, heating, three-point bending, heating-cooling cycle

Introduction

Fracture is a failure mechanism in brittle materials and is a very important phenomenon in the structures. Fracture has received much attention due to safety reduction, disruption or cessation of mining and construction activities in large-scale geotechnical operations and mining and civil engineering structures [1]. The fracture toughness is a property indicating the critical stress intensity factor. This critical value is shown by K_c. During loading when the stress intensity factor reaches a critical value, cracks begin to propagate (Figure 1).

There are three main stress modes for applying stress on the cracks including opening (Mode I), shearing and sliding (Mode II) and sliding and tearing (Mode III). Figure 2 schematically shows different fracture modes. Any combination of the three main modes is known as mixed mode.

[DOR: 20.1001.1.22286837.1398.13.5.6.5]

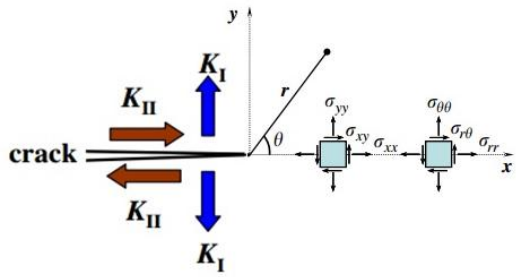

Figure 1. Polar coordinates of the crack tip and two main modes of crack propagation [2]

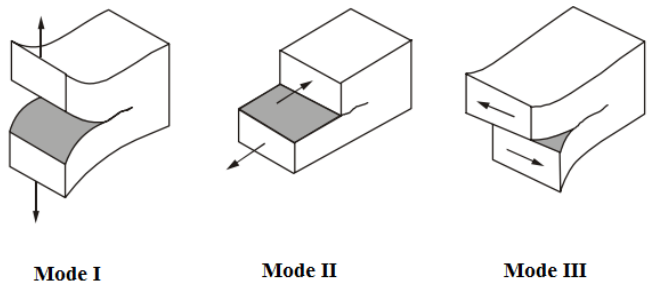

Figure 2. The main fracture modes [3]

Fracture toughness is used in many areas including hydraulic fracturing, rock explosion, rock cutting, design of underground spaces and rock fracture in mineral processing. Therefore, accurate determination of fracture toughness is of utmost importance. Fracture toughness is dependent on temperature, rate of loading, material composition and microstructure as well as geometric effects. All rocks are weak in tension. For this reason, Mode I (tensile mode) is the most critical loading mode. In cases such as explosion, fire, deep drilling and geothermal energy extraction, rocks are exposed to high temperatures influencing the rock toughness. Thus, the aim of this study is to investigate the effect of temperature on the fracture

[DOR: 20.1001.1.22286837.1398.13.5.6.5]

toughness of rocks. In this study, the effect of temperature on the mode I fracture toughness is investigated.

To determine the mode I fracture toughness, four tests have been standardized by the International Society for Rock Mechanics including short rod specimens [4], [5], chevron notched bend rod specimen, chevron notched Brazilian disk [6], [7] and three-point bending test on semicircle specimens [8], [9].

Many studies have been conducted on the effect of temperature on the rock properties. But there are few studies on the effect of temperature on mode I fracture toughness (Table 1). According to literature, the results of experiments do not depend only on the temperature, but the heating rate, the number of heating-cooling cycles and the concentration of micro-cracks also affect the test results [10].

Compared to the previous studies, the distinct features of this research are:

a) The first study on the the effect of the heating-cooling process on the mode I fracture toughness in Iran.
b) Use CT scan images to calculate the damage caused by heating-cooling process.
c) Type of rock studied.
d) Type of the test.

From the type of rock perspective, In addition to the natural specimens (includin sand stone, tuff, limestone and andesite), the

[DOR: 20.1001.1.22286837.1398.13.5.6.5]

concrete specimens used in the tunnel lining were also studied. While most of the past research has been done on sandstone.

From the type of the test perspective, this research has been investigated the effect of the heating-cooling process on the mode I fracture toughness, and in addition to the low temperatures, the effect of high temperature in the heating process and then the cooling of the specimen has been also studied on this mode. While most of the past researchs have only investigated the effect of low tempereture (during only the heating process, but not during the heating- cooling process) on the mode I fracture toughness. The effect of fire on the mode I fracture toughness was investigated. For this purpose, the specimens were heated to 700 $^{\circ}$C with the same heating rate in fire accidents. To determine the mode I fracture toughness, the three-point bending tests were performed on semicircular specimens. The test was conducted at six different temperatures (ambient temperature, 100, 200, 300, 500 and 700 $^{\circ}$C). To this end, the rock specimens were first heated and then naturally cooled to reach the ambient temperature. After cooling the semicircular specimens, an artificial notch was created and then the three-point bending tests were performed.

Specimen characteristics

1. Microscopic studies

The sandstone samples have been taken from Lalun formation in Loshan area and the Tuff from Karaj formation on Chalous Road and the limestone from the Abyek area, located 50 kilometers west of the

[DOR: 20.1001.1.22286837.1398.13.5.6.5]

Table 1. Studies on the effect of temperature on the mode I fracture toughness

References	Rock type	Test method	Main findings
[11]	limestone	Straight noched Brazilian disk specimen under diametrical compression	Up to a temperature range of 100 °C, the fracture toughness Increased the fracture toughness up to 100 °C and above 100 °C, the fracture toughness decreased.
[12]	Kimachi sandstone Tage tuff	single edge-notched round bar in bending (SENRBB) and three-point bending tests on semi-circular bend (SCB) specimens	No significant change was observed in the fracture toughness of Kimachi sandstone up to 125 °C. At higher temperatures, the fracture toughness increased with increasing temperature The fracture toughness of tuff decreased with temperature up to 75°C, whereas it increased above 100°C.
[13]	Laurentin Granite	Notched semi-circular bend, the dynamic load exerted by a modified split Hopkinson pressure bar (SHPB) system	The dynamic fracture toughness decreases with the treatment temperature when the temperature is higher than 250 °C.
[14]	Coconino sandstone	edge notched disc (END) tests	The fracture toughness decreases from an unheated value of about 0.7 to about 0.6 MPa√m when heated to 300 °C.
[15]	Manoharpur sandstone Bellary dolerite, Dholpur sandstone	three-point bending tests on semi-circular (SCB) specimens	Up to a temperature range of 100 °C, the fracture toughness of Manoharpur sandstone, Bellary dolerite and holpur sandstone increased by 40%, 25% and 65%, respectively, when compared to the ambient condition, and thereafter decreased with a gradual increase of temperature. At 600 °C, when compared to the ambient condition, the fracture toughness of these rock types decreased by 59%, 36% and 30% for Manoharpur sandstone, Bellary dolerite and Dholpur sandstone, respectively.
[16]	Concrete	The notched semi-circular bend specimens, the dynamic load exerted by a modified split Hopkinson pressure bar (SHPB) system	The dynamic fracture toughness deceases with the heat-treatment temperatures.

[DOR: 20.1001.1.22286837.1398.13.5.6.5]

city of Karaj, are located near the Tehran highway in Qazvin, Alborz province and the andesite from dikes in Qazvin province and southwest of the city of Buin Zahra.

For microscopic studies, thin sections were prepared from the rock specimens to take microscopic images shown in Figure 3.

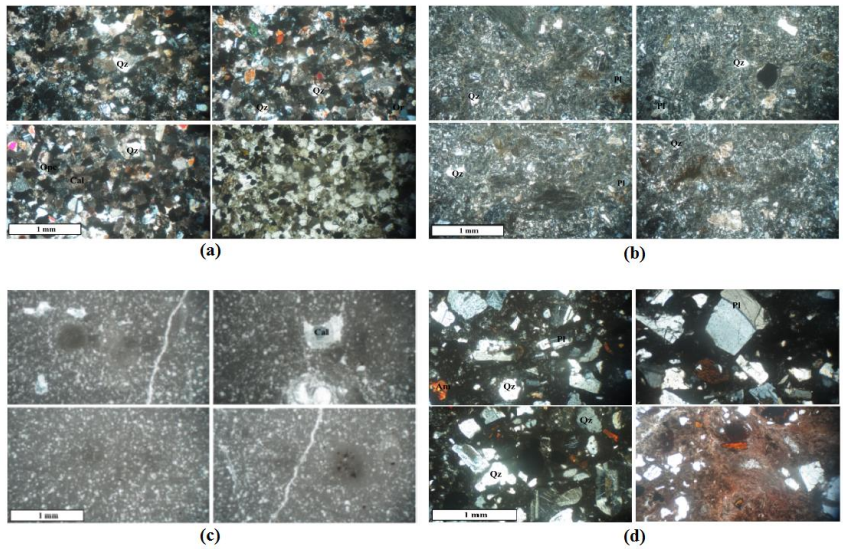

Figure 3. Microscopic images of four rock specimens, a) sandstone, b) tuff, c) limestone and d) andesite

The Figure 3 (a) is a section of sedimentary rock (sandstone). Shaped and semi-shaped quartz together with calcite are the main components of this rock. Primary and secondary minerals forming this rock are calcite, alkaline feldspar, quartz, and opaque minerals. The Figure 3(b) is a cross-section of an andesitic tuff that has been strongly silicified. Shaped and semi-shaped Cerrusite and calcified plagioclase in a silicified field are the main components of this rock.

[DOR: 20.1001.1.22286837.1398.13.5.6.5]

Minor minerals forming the rock include alkali feldspar, quartz, and opaque minerals. The Figure 3 (c) is limestone with a partially recrystallized microcrystalline calcite texture. The major mineral in this type of rock is calcite. The Figure 3 (d) is a section of andesite. Plagioclase makes up more than 50% of the rock crystals. Plagioclase crystals are usually shaped or semi-shaped, and can be zoned. The size of these crystals could reach 5.1 mm. The quartz and opaque minerals are of the most important minor minerals in the studied rocks.

2. X-ray diffraction (XRD) analysis

X-ray diffraction (XRD) analysis was used to identify the composition of the rocks. X-ray pattern was recorded from 2θ=10 to 80° with a step size of 0.02. The XRD data were analyzed with the help of EXPERT. Figure 4 shows the XRD patterns for four rock samples (sandstone, tuff, andesite and limestone).

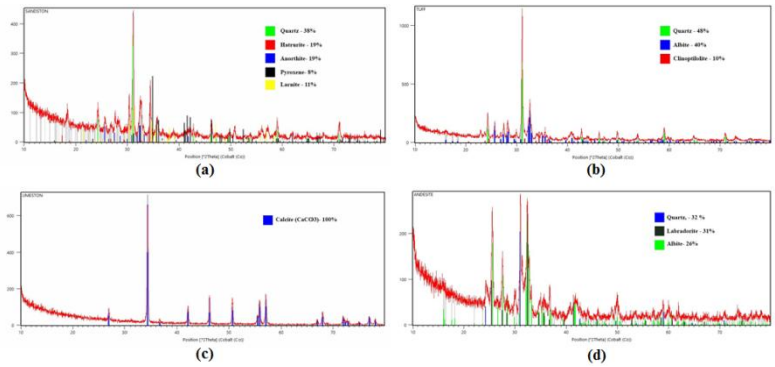

Figure 4. XRD patterns of for four rock samples, a) sandstone, b) tuff, c) limestone and d) andesite

[DOR: 20.1001.1.22286837.1398.13.5.6.5]

The phases in the sandstone sample include quartz (SiO_2), hatrurite (Ca_3SiO_5), anorthite (Ca [$Al_2Si_2O_8$]), pyroxene ([Ca-Na-Fe-Mg] Si_2O_6) and larnite ($Ca_2Si_2O_4$). The tuff rock sample contains quartz (SiO_2), albite ($NaAlSi_3O_8$) and clinoptilolite. The limestone sample contains calcite ($CaCO_3$). The phases in the andesite rock sample include quartz (SiO_2), labradorite ((Ca, Na) (Al, Si) $_4O_8$) and albite ($NaAlSi_3O_8$).

3. Physical and mechanical properties

Porosity is one of the most important physical properties of the rock with a significant influence on the mechanical parameters. In this research work, the density and porosity were determined based on the [17] standards. In order to better identify and understand the behavior of rocks, the mechanical properties of the rocks were determined according to American Society for Standard Testing and Materials (ASTM) and the International Society for Rock Mechanics (ISRM). These properties include uniaxial compressive strength [18] and indirect tensile strength [19]. Uniaxial compressive strength test was performed on all rock specimens to determine the uniaxial compressive strength and other elastic properties such as Young's modulus and Poisson's ratio. Table 2 shows the physical and mechanical properties of the specimens.

Table 2. The physical and mechanical properties of the specimens

Specimen	Uniaxial Compressive Strength (MPa)	Indirect tensile strength (MPa)	Young's modulus (GPa)	Poisson's ratio	Density (gr/cm3)	Effective Porosity (%)
Sandstone	77.62	8.34	17.77	0.25	2.38	9.84
Limestone	145.45	10.29	55.37	0.27	2.69	0.23
Andesite	143.63	10.69	34.55	0.2	2.23	3.6
Tuff	117.85	12.04	33.97	0.19	2.5	6.72

Specimen preparation

[DOR: 20.1001.1.22286837.1398.13.5.6.5]

The rock cores with a diameter of 73 mm were prepared from four rock blocks including andesite, tuff, limestone and sandstone from mines around Qazvin. The standard cores were prepared by slow drilling with caution. Water was used for cooling during drilling to prevent damages to the specimens and the device. A series of concrete specimens with a diameter of 71 mm and a water-cement ratio of 0.5 and equal amount of sand and cement was also prepared.

To prepare circular discs for the three-point bending tests on semicircular specimens, standard cores with a thickness of 30 mm were cut using a diamond cutting blade with high precision. In the cutting process, the plate from cutting the discs should not have an angle more than 0.5 perpendicular to the axis of the core [9].

The circular disks should be divided into two equal disks. The final stage is to create a notch in the specimens. To prevent the effect of heat on the notch, the specimens were first heat treated and then the notches were created.

The notches were created with a thin cutting blade. First, the semicircular specimens were fixed in a mold. To ensure vertical notches, the specimens were balanced. A crack of 15 mm length was created considering the cut portion (Figure 5). The notch length is selected so that the dimensionless ratio of the notch length to the radius of the specimen ranges from 0.4 to 0.6 ($0.4 \leq a / R \leq 0.6$).

[DOR: 20.1001.1.22286837.1398.13.5.6.5]

Figure 5. Notching the rock specimens

Figure 6 schematically shows the preparation steps. Table 3 shows the dimensions of the standard specimens.

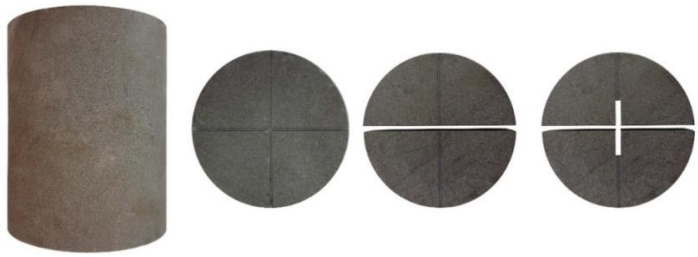

Figure 6. Preparation of the SCB specimen

Table 3. Suggested geometric dimensions of SCB [9]

Dimensions	Range
Diameter (D)	Larger than 10 times the average size of grains or at least 76 mm
Thickness (B)	Larger than 0.4D or 30 mm
Notch length (a)	$0.4 \leq a/R(=\beta) \leq 0.6$
Support length (s)	$0.5 \leq s/2R \leq 0.8$

Test methods

The tests on the semicircular specimens includes two steps: 1) heat treatment and 2) three-point bending tests

1. Heating-cooling cycle on natural and concrete specimens

The tests were performed on the prepared rock specimens. The experiments were conducted on a series of rock and concrete

[DOR: 20.1001.1.22286837.1398.13.5.6.5]

specimens heated to 100, 200, 300, 500 and 700 °C. A series of experiments was performed on unheated specimens. A programmable electric furnace was used for heat treatment. The heating rate (°C/min) and the residence time at a certain temperature can be adjusted. The heating rate in the electrical furnace was 15 °C to simulate fire and the rock behavior in accordance with a study by Mohtadi *et al*. on fire in Sadaf Commercial Complex in Qeshm [20]. After placing the specimens at a certain temperature, heating was stopped and the specimens were removed from the furnace to be naturally cooled to the ambient temperature. Thereafter, a notch was created on the specimens to be prepared for the tests. Figure 7 shows the placement of the specimens in the electric furnace.

Figure 7. The placement of the specimens in the electric furnace

2. The three-point bending test on the semicircular specimens

In this study, a hydraulic servo-control testing machine was used to perform the three point bending test on the specimens. Figure 8 shows the loading equipment on the SCB.

[DOR: 20.1001.1.22286837.1398.13.5.6.5]

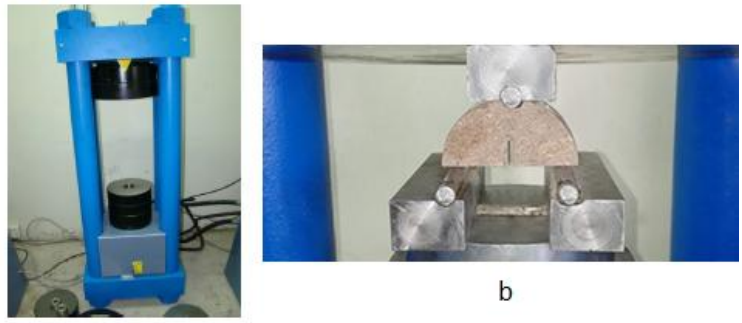

a b

Figure 8. a) Loading machine b) Loading equipment on SCB

The mode I fracture toughness (K_{Ic}) is calculated from equation (1) using the peak load obtained in the experiment [9].

$$K_{Ic} = Y' \frac{P_{max}\sqrt{\pi a}}{2RB} \quad (1)$$

Y' is obtained from equation (2).

$$Y' = -1.297 + 9.516\left(\frac{s}{2R}\right) - \left(0.47 + 16.457\left(\frac{s}{2R}\right)\right)\beta + (1.071 + 34.401(s/2R))\beta^2 \quad (2)$$

$$\beta = \frac{a}{R} \quad (3)$$

Equation (2) is used to determine the dimensionless stress intensity factor. This equation is obtained using the finite element method assuming plane strain condition.

5. Results and Discussion

Figure 9 shows the failure pattern of rock specimens used in the tests.

[DOR: 20.1001.1.22286837.1398.13.5.6.5]

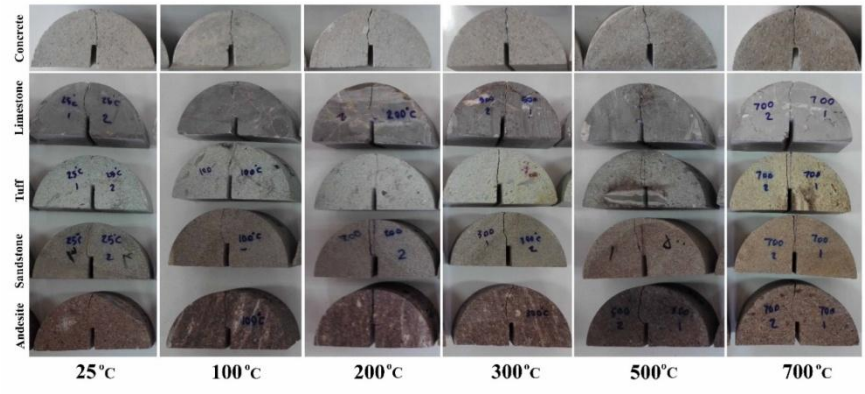

Figure 9. The rock specimens used in the tests (from top to bottom: concrete, limestone, tuff, sandstone and andesite)

The mode I fracture toughness for tuff, limestone, sandstone and andesite specimens was determined at 25 °C (ambient temperature) and at 100, 200, 300, 500 and 700 °C. The mode I fracture toughness for the tuff, limestone, sandstone and andesite specimens heated at 100 °C respectively decreased by 22, 13, 8.6 and 2.3% compared with unheated specimens. The mode I fracture toughness for the tuff, limestone, sandstone and andesite specimens heated at 200 °C respectively decreased by 11.5, 7.5, 14.6 and 3% compared with those heated at 100 °C. Table 4 shows the results of the mode I fracture toughness test, effective porosity and weight loss for the specimens after a heating-cooling cycle.

[DOR: 20.1001.1.22286837.1398.13.5.6.5]

Table 4. The results of the mode I fracture toughness test, effective porosity and weight loss for the specimens after a heating-cooling cycle

Specimen	Temperature (°C)	Effective Porosity (%)	Weight Loss (%)	Fracture toughness (MPa m1/2)
Sandstone1	25	9.84	0	0.928
Sandstone2	100	11.12	0.318	0.848
Sandstone3	200	11.17	0.559	0.724
Sandstone4	300	11.01	1.532	0.761
Sandstone5	500	11.34	2.256	0.671
Sandstone6	700	13.33	3.245	0.506
Andesite1	25	-	-	1.811
Andesite2	100	-	-	1.768
Andesite3	200	-	-	1.715
Andesite4	300	-	-	1.850
Andesite5	500	-	-	1.611
Andesite6	700	-	-	1.638
Limestone1	25	0.23	0	0.953
Limestone2	100	0.25	0	0.876
Limestone3	200	0.26	0.014	0.810
Limestone4	300	0.22	0.023	1.002
Limestone5	500	1.34	0.059	0.912
Limestone6	700	4.01	0.176	0.561
Tuff1	25	6.72	0	1.649
Tuff2	100	7.84	0.372	1.282
Tuff3	200	8.21	0.432	1.134
Tuff4	300	8.15	1.482	1.526
Tuff5	500	7.19	1.593	1.573
Tuff6	700	8.46	2.288	1.369
Concrete1	25	-	-	0.226
Concrete2	100	-	-	0.244
Concrete3	200	-	-	0.284
Concrete4	300	-	-	0.204
Concrete5	500	-	-	0.164
Concrete6	700	-	-	0.141

Figure 10 shows the mode I fracture toughness for andesite, tuff, limestone, and sandstone at different temperatures.

The mode I fracture toughness changes because the cracks density changes. The changes in the effective porosity and weight loss confirm

[DOR: 20.1001.1.22286837.1398.13.5.6.5]

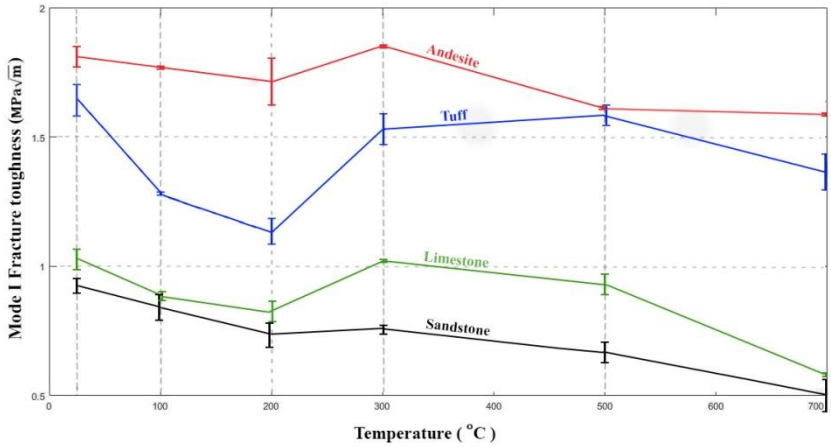

Figure 10. The mode I fracture toughness of andesite stone, tuff, limestone and sandstone at different temperatures

changes in the crack density. The variations of the cracks density are due to different thermal expansion coefficient of minerals. This coefficient is dependent to the mineralogy composition. Only in high temperature the physical and the mineralogical changes occur in the rock.

The more explanations are presented in the following paragraphs.

Toughness reduction at 100 °C or more generally in the range of 25 to 200 °C is inversely proportional to the grain size. This means that fracture toughness further decreases in fine-grained rock specimens.

This Temperature rise causes thermal stress in the rocks. Given different thermal expansion coefficients of different minerals, the stress is concentrated on the boundary of different minerals. If the stress exceeds the shear or tensile strength of the rocks, new cracks

[DOR: 20.1001.1.22286837.1398.13.5.6.5]

are formed or previous cracks increase. This is consistent with the results of Zhao *et al.* [21]. Furthermore, new cracks are formed especially at the grain boundaries of different minerals during cooling process due to contraction of the specimens. Thus, the crack density increases leading to a decrease in the mode I toughness fracture of the rock specimens. The grain size is related to the grain boundary cracks so that more cracks are observed in fine-grained rock specimens. For comparing the grain size of rock specimen, Figure 11 shows the images of the cross sections of coarse-grained and fine-grained rock specimens (from left to right).

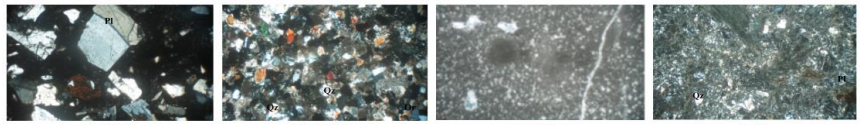

Figure 11. Thin sections of four rock specimens (from left to right: a) andesite, b) sandstone, c) limestone, and d) tuff)

The fracture toughness increases from 200 to 300 °C compared to 200 °C. The increase in the fracture toughness of the tuff, limestone, and sandstone and andesite rock specimen is 35, 24, 5 and 8 percent, respectively. The increased fracture toughness can be attributed to closure of pre-existing cracks in the rock specimens. Because of the closure of the pre-existing cracks in the rock specimens, the porosity decreases from 200 to 300 °C. At temperatures above 300 °C, the thermal expansion coefficient of the rock-forming minerals and mineralogical changes in some rocks influence the mode I fracture toughness of rock specimens. The fracture toughness of limestone and sandstone decreases at 500 and 700 °C. The fracture toughness of

[DOR: 20.1001.1.22286837.1398.13.5.6.5]

andesite decreases from 300 to 500 °C. The fracture toughness slightly changes up to 700 °C and remains almost constant during the process. The fracture toughness of the tuff specimen slightly increases up to 500 °C and then decreases up to 700 °C.

For a better analysis of the rock behavior, the effective porosity, weight loss and changes in the fracture toughness of sandstone, limestone and tuff were examined at 25, 100, 200, 300, 500 and 700 °C. To better understand the behavior of rocks and to examine the relationship between the effective porosity, weight loss and fracture toughness, the rock specimens were individually examined. As seen in Figure 12, heating and cooling of the three types of rocks including sandstone, limestone and tuff result in changes in the effective porosity. The increase in the effective porosity is due to an increase in the number of micro-cracks with increasing temperature [22].

The fracture toughness decreases at 100 and 200 °C. The effective porosity increases in this range due to an increase in the number of cracks caused by thermal stress on the boundary of different minerals. The fracture toughness increases at 300 °C. As a result, the effective porosity decreases at 300 °C compared with 200 °C. The cracks created in the previous steps are closed and density of cracks in the rock specimens decreases. The increase in effective porosity and weigh loss from 300 to 700 °C indicates an increase in the number of micro-cracks resulting in a decrease in the fracture toughness. At temperatures above and below the melting point, significant microstructural changes occur in the rocks. For this reason, the

[DOR: 20.1001.1.22286837.1398.13.5.6.5]

weight loss will rise sharply at these temperatures. This is consistent with the results of Dwivedi *et al.*[23]. At these temperatures, new micro-cracks are formed and the pre-existing cracks in the rock propagate. At the same time, physical and mineralogical changes occur in the rock. Heat causes changes in the rocks including rock appearance such as increased brightness, delamination or darkening as well as damages to micro-crystals including micro-cracks. This is in good agreement with the results of previous studies [22], [24]. Figure 13 shows the changes in the sandstone appearance at 500 $^{\circ}$C.

The influence of the damage induced by the heat-treatment (at of 25 $^{\circ}$C , 200 $^{\circ}$C and 500 $^{\circ}$C) on the mode I fracture toughness of sandstone specimens were investigated by using the X-ray micro-CT technique.

The typical CT images of sandstone specimens under different heat-treatment temperatures are shown in Figure 14. The darker zone illustrates low-density minerals and the lighter zone indicates high-density minerals [25]. There is no visible difference between these images. Therefore, a proper parameter to quantify the state of the sample is needed. This parameter is the CT value. The CT value (Hounsfield radiological density) is calculated from the gray-level data and scaled with the standard materials (-1000 Hu for air and 0 Hu for pure water) [26]. Thus, the CT value of the sample reflects the composition and micro-structure in the material.

The damage variable (D) is used to describe the damage induced by the heat-treatment based on the average CT values [27]:

$$D = \frac{H_0 - H}{H_0} \quad (4)$$

[DOR: 20.1001.1.22286837.1398.13.5.6.5]

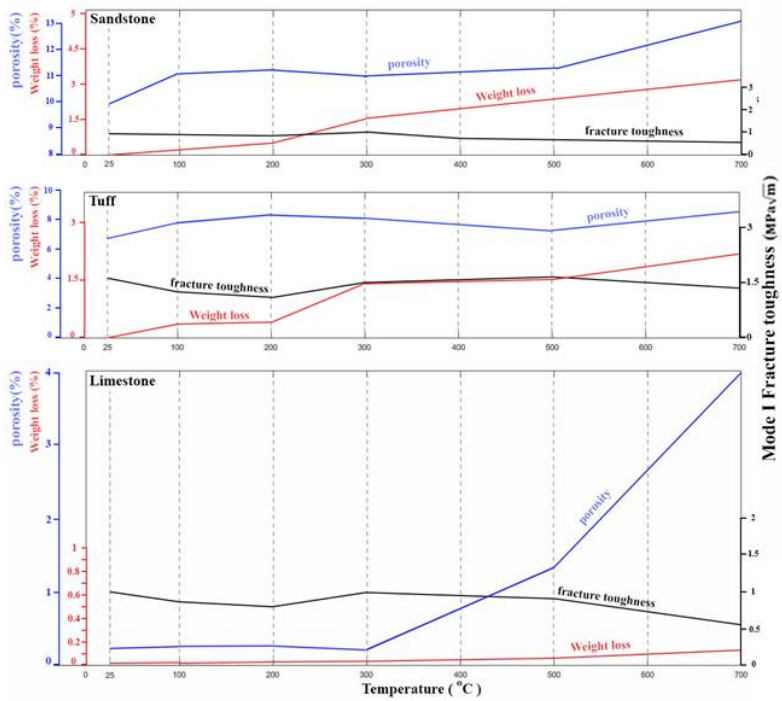

Figure 12. The changes in the fracture toughness, weight loss and effective porosity of sandstone, tuff and limestone at different temperatures

Figure 13. The cross-section of the sandstone specimen, a) at ambient temperature b) at 500 ˚C

Where H is the average CT value of heat-treated sample and H_0 is the average CT value of room temperature sample.

[DOR: 20.1001.1.22286837.1398.13.5.6.5]

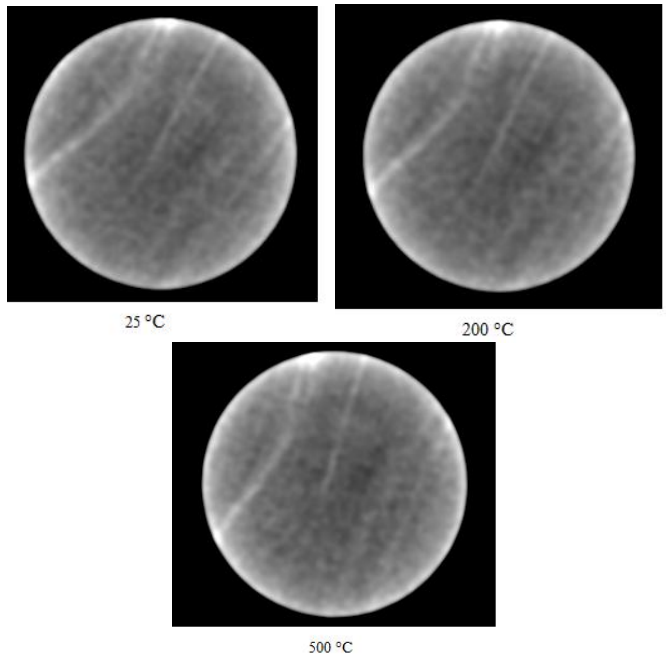

Figure 14. Typical CT images of sandstone samples under various heat-treatment temperatures

The calculated values of damage variable (D) are given in Table 5. It is shown that the values of damage variable of sandstone increase with the heat-treatment temperatures. These results are consistent with those obtained by Huang et al. (2015) and Yao et al. (2017).

Table 5. Average CT value and damage variable of sandstone samples under various heat-treatment temperatures

Heat-treatment temperature (°C)	Average CT value (Hu)	Damage variable (%)
25	1770	0
200	1739	1.75
500	1687	4.68

The tests conducted on the concrete specimens indicated an increase in the fracture toughness at 100 and 200 °C. This increase

[DOR: 20.1001.1.22286837.1398.13.5.6.5]

can be attributed to the reduced moisture content of the rock as well as micro-crack closure as a result of thermal expansion of the constituent particles of the concrete specimens. The fracture toughness of the concrete specimen decreased at 300, 500, and 700 °C due to increased expansion of the constituent particles and different coefficient of thermal expansion causing non-uniform contraction of the particles and formation of new micro-cracks in the concrete specimen. These micro-cracks reduce the fracture toughness at these temperatures. Figure 15 shows the mode I fracture toughness of the concrete specimen at different temperatures.

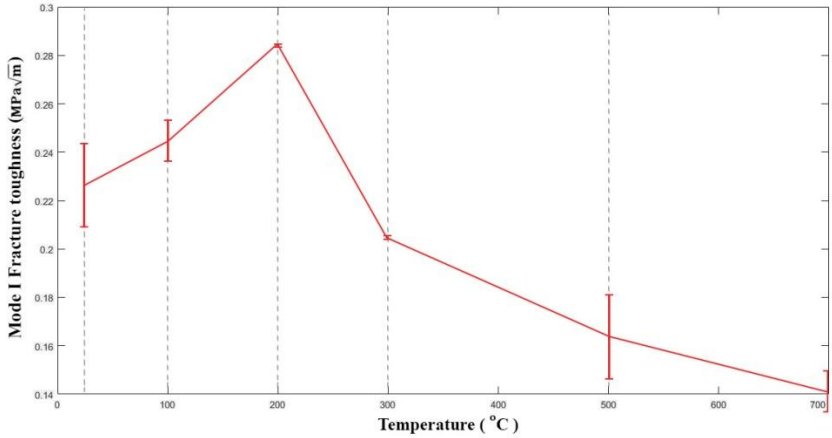

Figure 15. The fracture toughness of the concrete specimen at different temperatures

Conclusion

The effect of temperature on the mode I fracture toughness of four types of rocks including sandstone, limestone, tuff and andesite was investigated. For this purpose, the rock specimens were heated to

[DOR: 20.1001.1.22286837.1398.13.5.6.5]

100, 200, 300, 500 and 700 °C and then were cooled to ambient temperature. Comparison of the results showed that the constituent minerals affect the impact of heat on the mode I fracture toughness. The rocks and constituent minerals undergo changes when exposed to heat. These changes also affect the fracture toughness.

The second parameter is the grain size and different thermal expansion coefficient of minerals. Thus, more grain-boundary micro-cracks are formed in fine-grained rocks by applying heat due to different thermal expansion coefficient of the minerals. The number of micro-cracks is inversely correlated with the fracture toughness. As a result, the fracture toughness of fine-grained rocks is more significantly changed with temperature.

The main factor that causes changes in the mode I fracture toughness is the changes in the cracks density. The cracks desity changes occur because of different thermal expansion coefficient of minerals, grain size and mineralogy composition. For considering the variations of the cracks density, effective porosity and weight loss were determined in this research. The changes in the effective porosity and fracture toughness showed that these two parameters are inversely correlated. So reducing the effective porosity increased the fracture toughness. In contrast, the fracture toughness decreased with increasing the effective porosity.

Weight loss occurs in the heating-cooling process due to decomposition, removal of volatiles and structural water evaporation.

[DOR: 20.1001.1.22286837.1398.13.5.6.5]

According to the results, the fracture toughness decreased with increasing weight loss.

In this paper, the damage variable for sandstone specimens at each temperature was calculated using the average CT value to describe the damage due to heat-treatment. The results indicate the CT value decreases with the increase of the heat-treatment temperature. These can be explained by the evolution of micro-structures, i.e. the increase of micro-cracks and the undesirable chemical changes in the sandstone specimens.

References

1. Brace W. D., Bombolakis E. G., "A note on brittle crack growth in compression", Journal of Geophysical Research, 68(12) (1963) 3709-3713.

10. Chang S. H., Lee, C. I., Jeon S., "Measurement of rock fracture toughness under modes I and II and mixed-mode conditions by using disc-type specimens", Engineering geology, 66(1) (2002) 79-97.

2. Rao Q., Sun Z., Stephansson O., Li C., Stillborg B., "Shear fracture (Mode II) of brittle rock", International Journal of Rock Mechanics and Mining Sciences, 40(3) (2003) 355-375.

3. Hudson John A., Harrison John P., "Engineering rock mechanics", Elsevier Ltd (1997).

4. Barker L. M., "A simplified method for measuring plane strain fracture toughness", Engineering Fracture Mechanics, 9(2) (1977) 361-369.

[DOR: 20.1001.1.22286837.1398.13.5.6.5]

5. Ouchterlony F., "ISRM suggested methods for determining fracture toughness of rocks", Int. J. Rock Mech. Min. Sci. Geomech, Abstr. 25, (1988) 71-96.

6. Sheity D. K., Rosenfield A. R., Duckworth W. H., "Fracture toughness of ceramics measured by a chevron-notch diametral-compression test", Journal of the American Ceramic Society, 68 (12) (1985).

7. Fowell R. J., "January. Suggested method for determining mode I fracture toughness using cracked chevron notched Brazilian disc (CCNBD) specimens", In International Journal of Rock Mechanics and Mining Sciences & Geomechanics Abstracts, Vol. 32, No. 1, (1995) 57-64, Pergamon.

8. Lim I. L., Johnston I. W., Choi S. K., Boland J. N., June., "Fracture testing of a soft rock with semi-circular specimens under three-point bending. Part 1-mode I", In International journal of rock mechanics and mining sciences & geomechanics abstracts, Vol. 31, No. 3, (1994) 185-197, Pergamon.

9. Kuruppu M. D., Obara Y., Ayatollahi M. R., Chong K. P., Funatsu T., "ISRM-suggested method for determining the mode I static fracture toughness using semi-circular bend specimen", Rock Mech Rock Eng, 47 (2014) 267-274.

10. Meredith P. G., Atkinson B. K., "Stress corrosion and acoustic emission during tensile crack propagation in Whin Sill dolerite and other basic rocks", Geophysical Journal International, 75 (1) (1983) 1-21.

11. Al-Shayea N. A., Khan K., Abduljauwad S. N., "Effects of confining pressure and temperature on mixed-mode (I–II) fracture toughness of a

[DOR: 20.1001.1.22286837.1398.13.5.6.5]

limestone rock", International Journal of Rock Mechanics and Mining Sciences, 37 (4) (2000) 629-643.

12. Funatsu T., Seto M., Shimada H., Matsui K., Kuruppu M., "Combined effects of increasing temperature and confining pressure on the fracture toughness of clay bearing rocks", International Journal of Rock Mechanics and Mining Sciences, 41(6) (2004) 927-938.
13. Yin T., Li X., Xia K., Huang S., "Effect of Thermal Treatment on the Dynamic Fracture Toughness of Laurentian Granite", Rock Mech. And Rock Eng., 45 (6) (2012) 1087-1094.
14. Kim K., Kemeny J., Nickerson M., "Effect of rapid thermal cooling on mechanical rock properties", Rock Mechanics and Rock Engineering, 47(6) (2014) 2005-2019.
15. Mahanta B., Singh T. N., Ranjith P. G., "Influence of thermal treatment on mode I fracture toughness of certain Indian rocks", Engineering Geology, 210, (2016) 103-114.
16. Yao W., Xu Y., Liu H., Xia K., "Quantification of thermally induced damage and its effect on dynamic fracture toughness of two mortars", Engineering Fracture Mechanics, 169 (2017a) 74-88.
17. International Society for Rock Mechanics and Ulusay, R., "The complete ISRM suggested methods for rock characterization, testing and monitoring", 1974-2006. International Soc. for Rock Mechanics (2007).
18. Standard, A.S.T.M., 2010. D7012–10 (2010) "Standard test method for compressive strength and elastic moduli of intact rock core specimens under varying states of stress and temperatures", Annual Book of ASTM

[DOR: 20.1001.1.22286837.1398.13.5.6.5]

Standards, American Society for Testing and Materials, West Conshohocken, PA, 495-498.

19. ASTM, D. 3967, "Standard Test Method for Splitting Tensile Strength of Intact Rock Core Specimens", ASTM International, West Conshohocken, PA(2008).
20. Mohtadi V. R, Mohtadi A. R., "The results of ultrasonic testing on the concrete structure damaged in a fire accident, Sadaf Commercial Complex, Qeshm", Civil Journal, Retrofitting and Improvement, No. 31, (2015) 79-83.
21. Zhao Z., "Thermal Influence on Mechanical Properties of Granite: A Microcracking Perspective", Rock Mechanics and Rock Engineering, 49(3) (2016) 747-762.
22. Balme M. R., Rocchi V., Jones C., Sammonds P. R., Meredith P. G., Boon S., "Fracture toughness measurements on igneous rocks using a high-pressure, high-temperature rock fracture mechanics cell", Journal of Volcanology and Geothermal Research, 132(2) (2004)159-172.
23. Dwivedi R. D., Goel R. K., Prasad V. V. R., Sinha A., "Thermo-mechanical properties of Indian and other granites", International Journal of Rock Mechanics and Mining Sciences, 45(3) (2008) 303-315.
24. Domanski M., Webb J., "A review of heat treatment research", Lithic technology, 32(2) (2007)153-194.
25. Yao W., Xu Y., Wang W., Kanopolous P., "Dependence of dynamic tensile strength of longyou sandstone on heat-treatment temperature and loading rate", Rock Mechanics and Rock Engineering, 49 (10) (2016) 3899-3915.

[DOR: 20.1001.1.22286837.1398.13.5.6.5]

26. Yao W., Liu H. W., Xu Y., Xia K., Zhu J., "Thermal degradation of dynamic compressive strength for two mortars", Construction and Building Materials, 136 (2017b) 139-152.

27. Huang S., Xia K., "Effect of heat-treatment on the dynamic compressive strength of Longyou sandstone", Engineering Geology, 191 (2015) 1-7.

[DOR: 20.1001.1.22286837.1398.13.5.6.5]